Pergamon

Journal of Structural Geology, Vol. 20, No. 11, pp. 1521 to 1530, 1998

PII: S0191-8141(98)00050-9

0191-8141/98/$ - see front matter

Determining finite longitudinal strains from oppositely-concave microfolds in and around porphyroblasts: a new quantitative method

S. E. JOHNSON

School of Earth Sciences, Macquarie University, Sydney, New South Wales 2109, Australia
E-mail: scott.johnson@mq.edu.au

and

M. L. WILLIAMS

Department of Geoscience, University of Massachusetts, Amherst, Massachusetts, 01003, U.S.A.

(*Received* 5 *September* 1997; *accepted in revised form* 12 *May* 1998)

Abstract—This paper describes a precise new method for determining finite longitudinal strains in porphyroblastic metamorphic rocks, which makes use of oppositely-concave microfolds (OCMs) formed by heterogeneous strain of the matrix around porphyroblasts. The initial spacing between two foliation surfaces is measured inside a porphyroblast and compared to the spacing between the same two surfaces in the matrix, which results in a measure of extension (e) experienced by the rock during and/or after porphyroblast nucleation. A natural example is provided by the well-known 'millipede' plagioclase porphyroblasts from the Robertson River Metamorphics in Queensland, Australia. Twenty-four measurements were made from 22 serial thin sections cut parallel to both the X–Z and X–Y planes of finite strain, giving an average extension of 1.72 parallel to the X-direction of finite strain. The least-squares best-fit line to a plot of initial length vs change in length gives an R^2 value of 0.998. A minimum estimate of maximum shortening (negative e) was also made by measuring the total lengths of S_1 folia that had been crenulated during OCM formation, giving a value of −0.54, which falls short of the −0.63 expected for constant-volume, plane-strain deformation. Because the OCM method is particularly suited to metapelites, results may provide new insight into mechanisms of folding and crenulation cleavage development, pressure–temperature–time-deformation histories, mass transport during deformation and metamorphism, and kinematic studies of porphyroblast behavior (rotation vs non-rotation) during ductile deformation. © 1998 Elsevier Science Ltd. All rights reserved

INTRODUCTION

Absolute measurements of finite longitudinal strains are a desirable component of many structural analyses, but appropriate strain markers are rare, owing to a general lack of knowledge regarding the pre-deformational shapes or dimensions of deformed objects. Extensions (e—also known as elongation) have been measured using stretched fossils such as belemnites, crinoids and graptolites, and stretched metamorphic crystals such as tourmaline and kyanite (e.g. Ramsay and Huber, 1983). With the exception of graptolites, where initial lengths are known, these techniques generally use measurements in the deformed state to constrain, or reconstruct, the original lengths. For example, if a fossil or mineral has been brittlely segmented, the initial length can be obtained by combining the measured lengths of the individual segments (e.g. Beach, 1979; Ramsay and Huber, 1983). Such measurements generally underestimate the total extension because they assume that the markers have not been internally strained, and because some ductile matrix deformation probably occurred before the initial segmentation of the markers (Beach, 1979). Furthermore, appropriate markers are rare in metapelites, which are some of the most useful rocks for metamorphic and microstructural analysis. This paper describes a new method for determining finite longitudinal strains in porphyroblast-bearing schists, making use of inclusion trails and the surrounding matrix foliations.

METHOD

Porphyroblasts containing inclusion trails that are continuous with matrix foliations are common in metamorphic rocks (e.g. Zwart, 1962; Fyson, 1980; Bell *et al.*, 1986; Vernon, 1989; Johnson, 1990; Passchier and Speck, 1994; Williams, 1994; Aerden, 1995; Davis, 1995). The strain analysis technique presented here is possible because inclusion trails preserve geometrical characteristics of a foliation at the time of porphyroblast growth, which can be compared to the present-day characteristics of that same foliation in the matrix. A particularly useful variety of inclusion trails is characterized by outwardly-opening, oppositely-concave microfolds (OCMs; Fig. 1). OCMs can be used to quantify longitudinal strains that occurred during and/or after porphyroblast growth, because the spacing

between any two inclusion trails inside the porphyroblast is different from the spacing between the same two foliation surfaces outside. Johnson and Bell (1996) have classified OCMs into five non-genetic types, based on geometry. The method described here is best applied to Types 2 and 3 (Fig. 1). In our experience, Types 2 and 3 are the most common OCMs (e.g. Passchier and Speck, 1994; Aerden, 1995; Johnson and Moore, 1996), and where we have observed them, the relationships between the porphyroblast inclusion trails and matrix foliations have been similar to those shown in Fig. 1.

Determining longitudinal strain in the X-direction of finite strain

Longitudinal strains can be quantitatively determined in a variety of orientations relative to the principal planes of finite strain. However, the X–Z plane (left-front faces in Fig. 1) provides an especially useful view of porphyroblast-matrix microstructural relationships, and is generally the easiest section in which to make the required measurements. An obvious advantage of this orientation is that it yields the X-direction of the strain ellipsoid. If a rock contains a well-developed mineral elongation lineation on the foliation formed during OCM development, the X–Z plane can be closely approximated as lying parallel to this lineation, and perpendicular to the contemporaneous foliation, as illustrated in the left-front faces in Fig. 1. Where the lineation is not pronounced in hand samples, or to provide a check on the above method, sections cut parallel to the X–Y plane (S_2 in Fig. 1) commonly show elongation of mica and quartz in the pressure/strain shadows adjacent to porphyroblasts (Fig. 1), which can be used to identify the X-direction. When the appropriate thin sections have been made, extensions in the X-direction of finite strain can be determined as shown in Fig. 2 using the definition

$$e = (l_f - l_i)/l_i$$

where l_f is the final length, and l_i is the initial length. l_i is obtained by measuring the separation of inclusion surfaces within the porphyroblast, and l_f by measuring the separation of the same two foliation surfaces well away from the porphyroblast. For convenience, negative values of extension are referred to below as *shortening*.

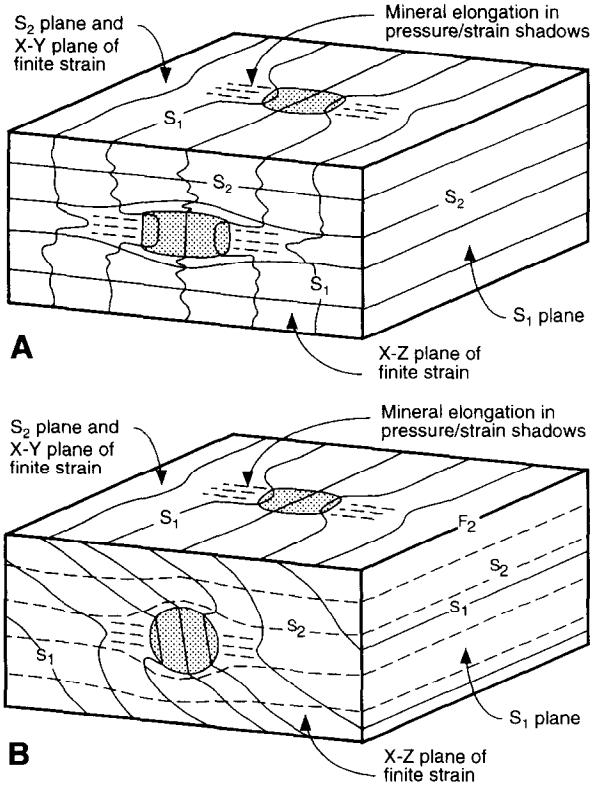

Fig. 1. Block diagrams showing the relationships between OCMs, porphyroblast inclusion trails, two foliations (S_1 and S_2) and F_2 fold axes. Dashed lines adjacent to porphyroblasts indicate the orientations of phyllosilicates and elongate quartz grains in the porphyroblast pressure/strain shadows. The OCMs occur either side of the porphyroblasts and are cored in the matrix by pressure/strain shadows. (a) Type 2, or symmetric OCMs. (b) Type 3, or asymmetric OCMs. Although we found no obvious problems using Type 3 OCMs, most OCMs used in this study were relatively symmetric.

Constraints on other principal strains

Depending on the specific microstructures available, it may also be possible to determine extensions in one or both of the other principal directions (Z and Y). Estimates of shortening in the Z-direction can be made in the same X–Z sections by comparing the total folded length of a crenulated folia, measured perpendicular to the syn-OCM foliation (S_2 in Fig. 1a), with the straight-line length. For example, the present S_2-perpendicular length of any S_1 folia in Fig. 1(a), compared to the unfolded length, gives an estimate of shortening. This can be done in numerous locations within the section to assess heterogeneity, but is generally only possible where the syn-OCM foliation is a crenulation cleavage, and where individual crenulated folia are distinct enough to be tracked through the crenulations. If a sufficient amount of shortening has occurred in the Y-direction of strain, a similar method can be used on sections cut parallel to the X–Y plane of strain (i.e. the top faces in Fig. 1). If the Y-direction has experienced positive extension, the magnitude of this strain may be impossible to quantify with the geometry shown in Fig. 1.

Assumptions and restrictions

Measurements of extension require continuity between the inclusion trails and matrix foliations so that individual foliation surfaces can be traced from the porphyroblast into the matrix. To obtain consist-

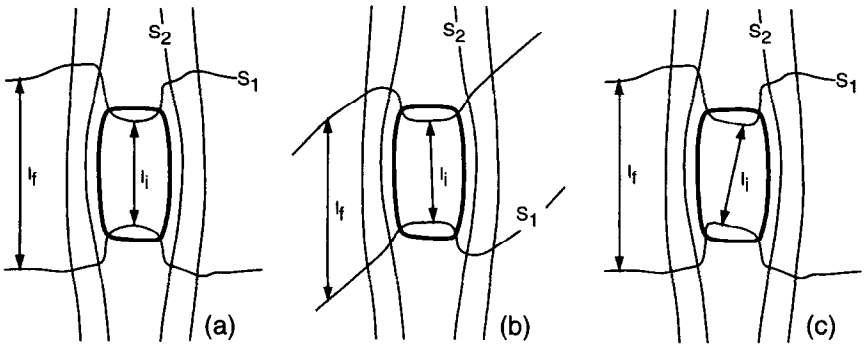

Fig. 2. Diagrams illustrating how measurements were made for calculating extensions. (a) S_1 and S_2 are orthogonal, and the values of l_i and l_f can be measured parallel to one another and S_2. (b) S_1 is oblique to the S_2 pole, and the values of l_i and l_f can be measured parallel to one another and S_2. (c) S_1 and S_2 are orthogonal, but the inclusion trails are oblique to both. In this instance l_i is measured orthogonal to the inclusion trails, and l_f parallel to S_2.

ent results from porphyroblast to porphyroblast in a single thin section or hand sample, l_f should be measured far enough from the porphyroblasts to avoid strain gradients near their margins. Additionally, all porphyroblasts evaluated must have grown at approximately the same time relative to the deformation that caused the OCMs; however, under special circumstances of sequential porphyroblast growth, the method can possibly provide estimates of strain at different points in the metamorphic history. Some porphyroblasts may contain inclusion trails significantly oblique to the same foliation in the matrix, or to inclusion trails in other porphyroblasts, but we have not found this to be a problem. Johnson and Bell (1996) have shown that the geometries in Fig. 1 reflect the strain state, and are independent of the degree of non-coaxiality during OCM development; thus, a knowledge of the deformation history is not required to apply the method described here. In X–Y sections (top faces in Fig. 1), the orientation of S_1 relative to S_2 cannot be fully determined, and so care must be taken when evaluating extensions in these sections.

NATURAL EXAMPLE

As a natural example, we evaluated an OCM-bearing sample from the Robertson River Metamorphics, Australia, which was originally described by Bell and Rubenach (1980), and subsequently serially thin-sectioned and computer-modelled by Johnson and Moore (1996; see the QuickTime movies at the URL: http://www.es.mq.edu.au/jmg/1996/1996.html). This sample contains plagioclase porphyroblasts in a matrix of quartz and muscovite, and the relationships between OCMs, porphyroblast inclusion trails, and two foliations are essentially identical to those shown in Fig. 1. Surfaces were cut parallel to S_2, which we assume was the X–Y plane of finite strain during OCM development, and the X-direction in this plane was determined using a mineral elongation lineation in hand sample. Seventy-five serial thin sections were then made, 69 parallel to the X–Z, and six parallel to the X–Y planes of finite strain for the syn-OCM deformation. Nineteen porphyroblasts were intersected in X–Z sections where matrix S_1 made a large angle with S_2, and inclusion trails could be clearly traced into the matrix. In addition, three useful porphyroblasts were intersected in thin sections cut parallel to the X–Y plane, all three from a thin-section block where S_1 was known to lie at a large angle to S_2.

Extensions determined parallel to the X-direction of finite strain

Extensions were determined parallel to the X-direction for the 22 intersected porphyroblasts using the method shown in Fig. 2. Three porphyroblasts are shown in Fig. 3 (accompanying line diagrams in Fig. 4) to illustrate the method, two from thin sections parallel to the X–Z plane of finite strain (Fig. 3a & b), and one from a thin section parallel to the X–Y plane (Fig. 3c). We used a 35 mm transparency film to photograph the porphyroblasts, and oriented the thin sections so that the long axes of the photographs were parallel to S_2 in X–Z sections, and perpendicular to S_1 in X–Y sections. Using color photocopy enlargements made from the transparencies, two well-spaced S_1 surfaces from inside each porphyroblast were carefully traced into the matrix (e.g. Fig. 4a–c). Two separate determinations were made for two of the porphyroblasts, using two separate sets of S_1 surfaces, giving a total of 24 measurements shown in Table 1 and Fig. 5. Extensions range from 1.63 to 1.77, with an average of 1.72 (Table 1 & Fig. 5). The data makes a strong linear trend on a plot of l_i against $(l_f - l_i)$, with an R^2 value of 0.998 (Fig. 6), indicating that the method is precise, and that the measurements are consistent with an average extension of 1.72 (the slope of the linear trendline). As argued by Bell and Rubenach (1980) and Johnson and Moore (1996), the cores of these porphyroblasts were either present prior to the onset of

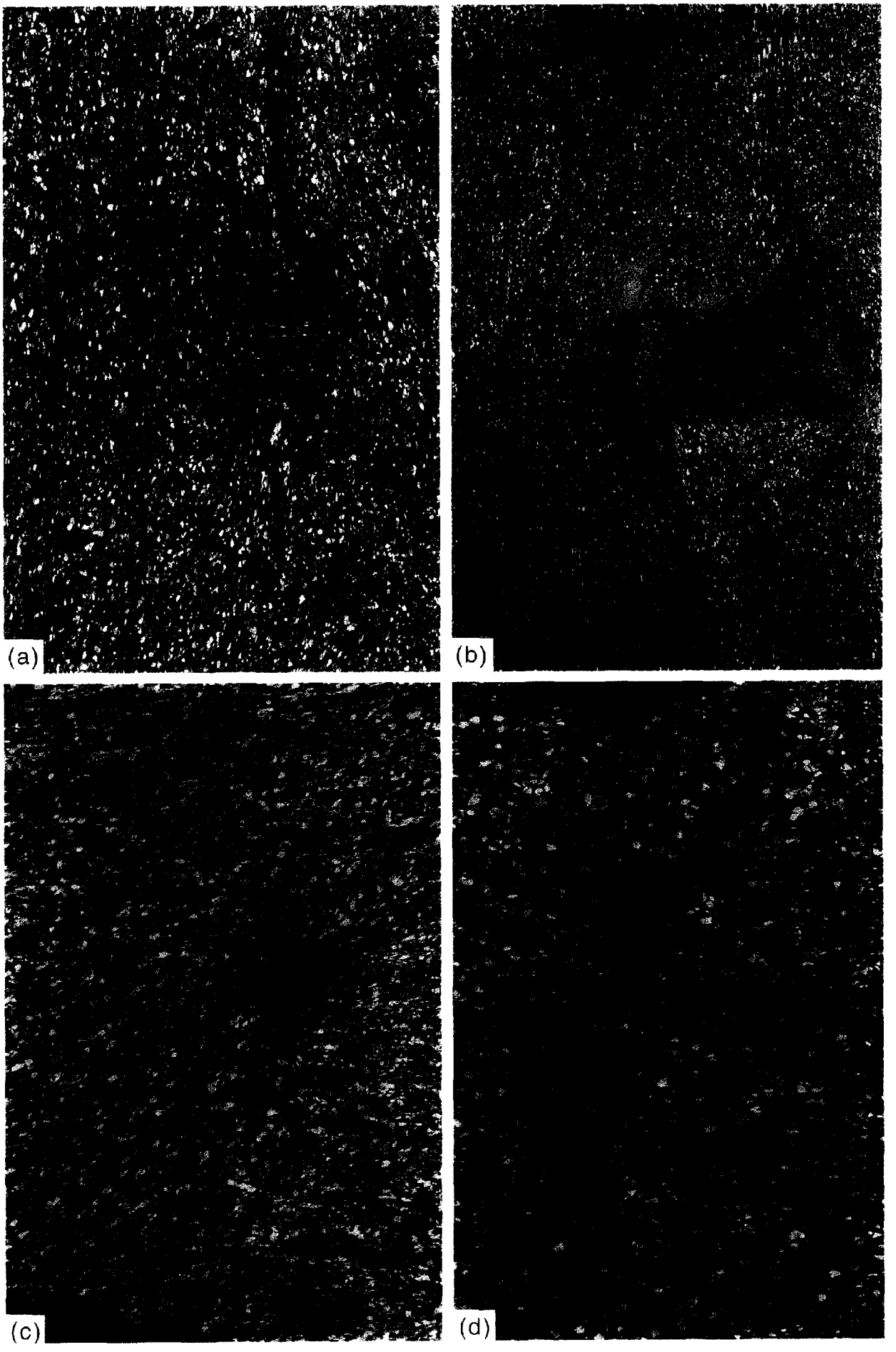

Fig. 3. (*caption opposite*).

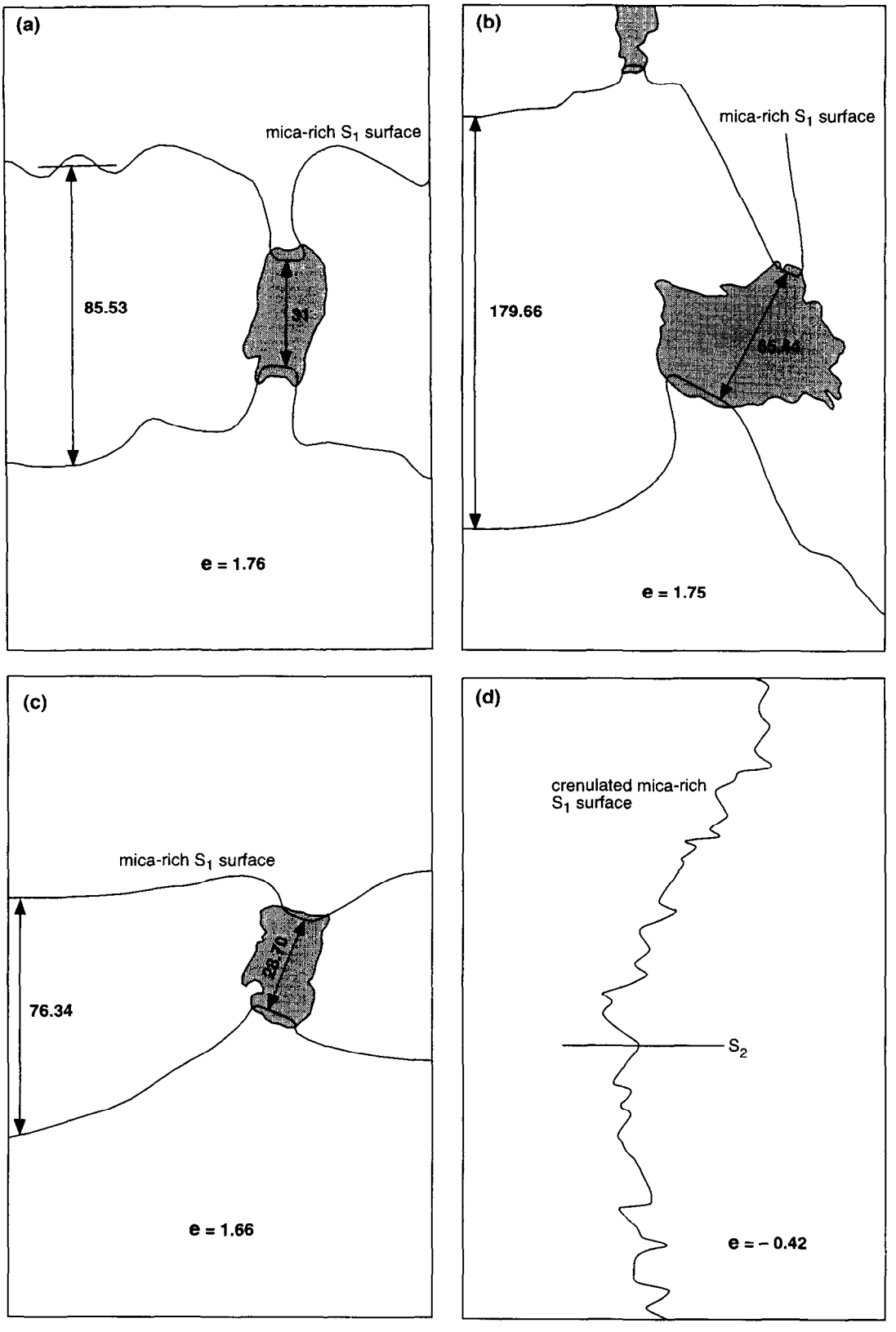

Fig. 4. Line-diagrams of the photomicrographs shown in Fig. 3, illustrating application of methods for calculating extension (a–c) and shortening (d).

Fig. 3. Photomicrographs showing microstructures used to calculate extension (a–c) and shortening (d). See Fig. 4 for accompanying line diagrams. (a) Porphyroblast elongate parallel to S_2, with inclusion trails parallel to matrix S_1. Thin Sections 1-8(a), cut parallel to X–Z plane of finite strain. Crossed polars, long axis 17.5 mm and parallel to S_2. (b) Porphyroblast with inclusion trails significantly oblique to matrix S_1. Thin Sections 1–9, cut parallel to X-Z plane of finite strain. Crossed polars, long axis 32 mm and parallel to S_2. (c) Porphyroblast in section X–Y (b), cut parallel to the X Y plane of finite strain. Because section is parallel to S_2, S_1 is the only obvious foliation, and l_f is measured perpendicular to S_1 in the matrix (Fig. 4c). Crossed polars, long axis 15 mm. (d) Crenulated mica-rich S_1 foliation surface. Thin Sections 1–3, crossed polars, long axis 11 mm and perpendicular to S_2.

Table 1. OCM extensions collected from 22 porphyroblasts in thin sections cut parallel to the X Z and Z Y planes of finite strain. Data ordered by initial-length (l_i) for plotting Figs 5 and 6. The l_i and l_f values are relative, and do not correspond to actual object lengths

Thin Section	l_i	l_f	(l_f-l_i)	Extension
8-9a	14	38	24	1.71
5-2b	14.35	38.46	24.11	1.68
4-10b(1)	17.79	48.79	31	1.74
X-Yc	18.95	51.76	32.81	1.73
1-7	20.09	53.38	33.29	1.67
4-8b	20.09	53.96	33.87	1.69
X-Ya	21.81	57.4	35.59	1.63
1-3	22.39	61.99	39.6	1.77
1-8b	24.79	67.07	42.28	1.71
1-5	28.13	76.92	48.79	1.73
5-2a	28.13	76.34	48.21	1.71
4-4	28.7	78.64	49.94	1.74
X-Yb	28.7	76.34	47.64	1.66
1-8a	31	85.53	54.53	1.76
4-10a	34.26	94.04	59.78	1.74
1-2	36.45	99.14	62.69	1.72
8-1	40.82	110.81	69.99	1.71
4-8a	41.33	111.36	70.03	1.69
8-9b	42	116	74	1.76
1-15	43.05	116.52	73.47	1.71
4-10b(2)	44.77	123.41	78.64	1.75
4-1	52.81	140.63	87.82	1.66
1-2	59.05	161.83	102.78	1.74
1-9	65.44	179.66	114.22	1.75

D_2, or grew very early during this syn-OCM deformation. The gentle curvature of inclusion trails in the porphyroblast rims suggests that the rims grew early during D_2. The cores account for most of the area of the porphyroblasts and for most of the length across the inclusion trails where l_i was measured (e.g. Fig. 3a–c), and this, combined with the early- or pre-D_2 growth of the cores, indicates that measured extensions probably reflect most of the finite extension experienced during D_2.

Extensions determined parallel to the Z- and Y-directions of finite strain

We also attempted to determine the magnitude of shortening in the Z-direction, using some of the same thin sections used for the above analysis. Eleven areas were photographed in the matrix of 10 separate thin sections containing mica-rich S_1 cleavage domains, the thin sections oriented so that the long axes of the photographs were perpendicular to S_2 (e.g. Figs 3d &

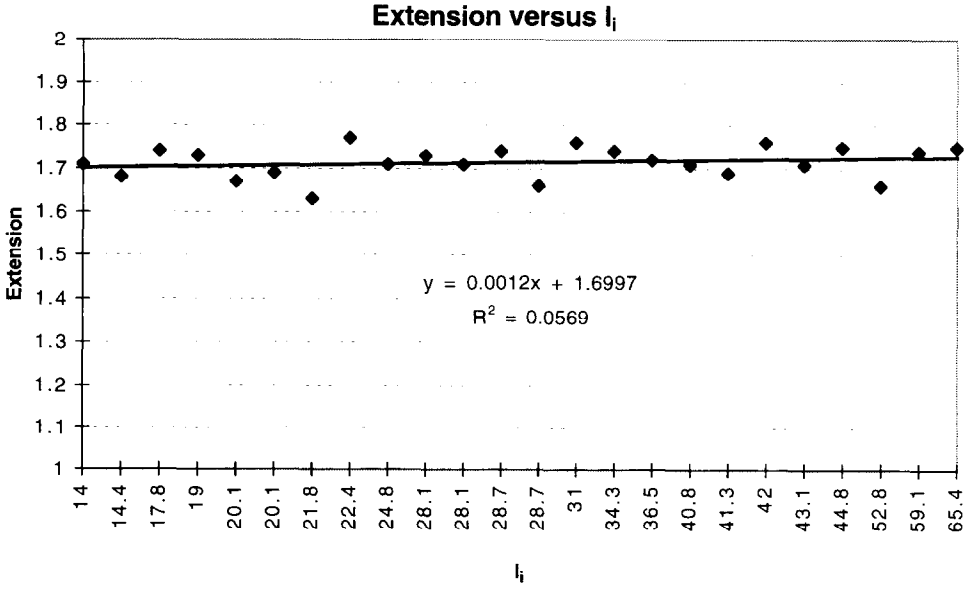

Fig. 5. Plot of extension vs l_i for 24 measurements made from 22 porphyroblasts (Table 1). Extension values range from 1.63 to 1.77, and average 1.72. Values of l_i are relative and do not correspond to actual object lengths.

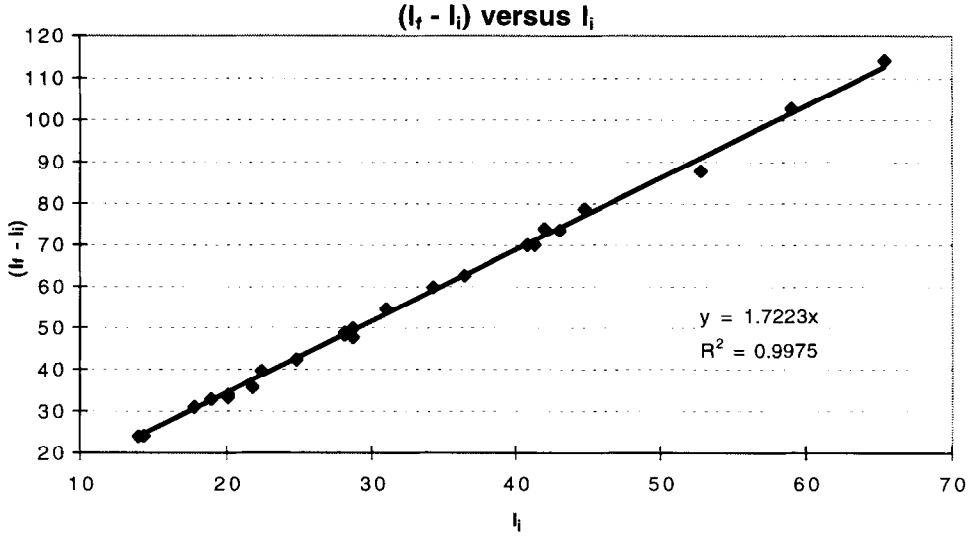

Fig. 6. Plot of l_f–l_i vs l_i for the porphyroblasts in Table 1 and Fig. 5. The data form a tight linear trend ($R^2 = 0.9975$), indicating that the method is precise, and the measurements are consistent with an average extension of 1.72 (the slope of the line). Values of l_i and (l_f–l_i) are relative, and do not correspond to actual object lengths.

4d). Using color photocopy enlargements from the transparencies, crenulated mica-rich S_1 domains were carefully traced, and a line parallel to S_2 was added (e.g. Fig. 4d). The margins of mica-rich S_1 domains were clearly modified during S_2 development, and so we traced mica orientations near the centers of the domains. The tracings were scanned, ensuring that the S_2 line on the tracing paper was approximately parallel to one of the edges of the scanner bed, and the image imported into Canvas 5.0™. S_1 domains were retraced using the polygon tool, and the object specifications dialogue box was used to determine the height (l_f) and perimeter (l_i) of the layer for the shortening calculation (Fig. 4d); shortening values ranged from −0.42 to −0.54 (Table 2 & Fig. 7).

The estimates of shortening in the Z-direction have a much larger scatter than positive-extension determinations from the same thin sections (compare Figs 5 & 6 with Fig. 7). This variation probably does not result from simple strain heterogeneity at the hand-sample scale (particularly if the deformation is a constant-volume process at that scale), because a similar degree of scatter would be expected in the extension data. The S_2 cleavage domains show variable amounts of quartz dissolution, illustrating the local volume redistribution typical during crenulation cleavage development. Additionally, S_2 cleavage domains at relatively early stages of their development commonly contain very-tight to isoclinal microfolds of S_1 cleavage domains, whereas in higher-strain sites the microfolds have been destroyed, and new mica grains have grown parallel to S_2 (Fig. 3d). We suggest that loss of S_1-length by destruction of these microfolds, combined with local volume loss from S_2 cleavage domains, is responsible for much of the variation in the measured shortening data. Additional loss of S_1-length may have occurred by dissolution and recrystallization along the old S_1 folia during layer-parallel shortening. From these considerations, our measurements underestimate the magnitude of shortening, and thus the value of −0.54 (Fig. 7) should be considered a minimum estimate of the bulk shortening in the Z-direction.

Table 2. Negative extensions (shortening) collected from crenulated S_1 cleavage domains in 10 thin sections cut parallel to the X–Z plane of finite strain (left-front faces of Fig. 1). Data ordered by shortening for plotting Fig. 7. The l_i and l_f values are relative, and do not correspond to actual object lengths

Thin Section	l_i	l_f	Shortening
4-4	23.89	10.94	−0.54
4-8	17.71	8.42	−0.52
1-2	11.24	5.60	−0.50
1-15(2)	20.10	10.20	−0.49
5-6	21.03	10.63	−0.49
8-1	17.64	9.26	−0.48
1-9	14.81	7.79	−0.47
4-1	15.18	8.05	−0.47
1-15(1)	17.66	9.73	−0.45
1-5	12.46	7.25	−0.42
1-3	17.22	10.05	−0.42

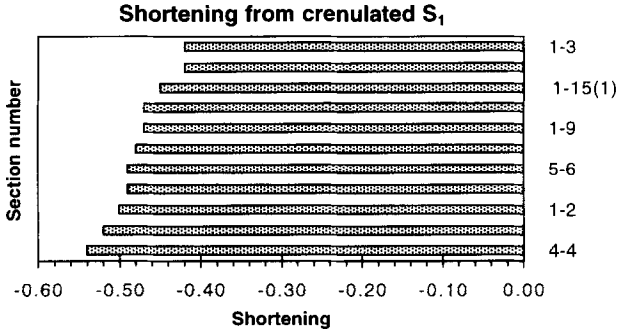

Fig. 7. Shortening values calculated from crenulated S_1 cleavage domains measured in 10 thin sections cut parallel to the X–Z plane of finite strain. We used this plot to determine a minimum value of −0.54 for the maximum bulk shortening strain.

Using thin sections cut parallel to the X–Y and Y–Z principal planes, we were unable to find convincing evidence for either positive or negative extension in the Y-direction of finite strain (e.g. Fig. 3c). We suggest that either the magnitude of this strain is too small to leave evidence such as microfolds, dissolution seams, or pressure/strain shadows parallel to the Y-direction adjacent to porphyroblasts, or that it was very homogeneous. If the deformation was plane-strain ($e_y = 0$) and constant-volume $[(1 + e_x)(1 + e_y)(1 + e_z) = 1]$ at the hand-sample scale, a value of −0.63 would be expected for shortening in the Z-direction. Our estimate of −0.54 falls short of this value, and so we suggest that some amount of shortening has probably occurred in the Y-direction. Assuming extension values of 1.72 and −0.54 in X- and Z-directions, respectively, a value of −0.20 in the Y-direction would be required for constant-volume strain. Twenty per cent shortening along Y might be recognizable if it caused microfolds of S_1 or dissolution seams, but if the strain was relatively homogeneous it would be difficult to separate the effects from those caused by strain in the X- and Z-directions.

An alternative to shortening in the Y-direction is that this sample has experienced a net volume increase (i.e. extension along X is not compensated by shortening along Y and/or Z). There is abundant evidence for dissolution of quartz and other components along crenulation seams, as well as evidence for addition of quartz in the pressure/strain shadows adjacent to porphyroblasts (Fig. 3a & b). However, we could not evaluate the degree to which these two processes compensate, and thus we could not evaluate bulk volume gain or loss. Nonetheless, we do not favor significant volume gain during bulk shortening of this rock during D_2, and so our preferred interpretation is that the deformation was nearly constant-volume, and that average shortening of from approximately −0.54 to −0.63, and from −0.20 to 0.0, occurred in the Z- and Y-directions, respectively.

DISCUSSION

Oppositely-concave microfolds (OCMs) provide a powerful method for estimating the absolute magnitude of extension in the X-direction of finite strain in deformed metapelitic rocks. OCMs fundamentally record strain in the matrix (after the time of porphyroblast nucleation), and so do not require assumptions or prior knowledge about the mechanical properties of the strain markers. Consequently, the OCM method can provide precise results with relatively few measurements (e.g. Figs. 5 & 6). Further, unlike other methods of evaluating matrix strains, for example the Fry method (e.g. Hanna and Fry, 1979), each marker can potentially yield several estimates of extension, which can be averaged or used as cross-checks. The method also provides a means for evaluating strain heterogeneity at various scales.

OCMs are especially useful strain markers because they tend to occur in porphyroblast-bearing metapelites, which are amenable to detailed metamorphic analysis. In particular, zoned porphyroblasts are typically used to place constraints on the shapes and locations of P–T t paths in metamorphic rocks (Spear, 1993). OCMs offer a potential link between the metamorphic and deformation histories, because strain magnitudes can be linked to a particular type of porphyroblast (e.g. staurolite, garnet or plagioclase), and so it may be possible to relate individual parts of the deformation history to individual stages in the metamorphic history. Also, it is increasingly possible to obtain precise geochronology from porphyroblasts (Christensen *et al.*, 1989, 1994; Vance and O'Nions, 1992; Lanzirotti and Hanson, 1997), rather than trace-phases such as zircon or monazite, and so it is possible to place absolute times on strain events, or even on stages in a strain history.

We emphasize that OCMs can provide absolute magnitudes of extensions in the X-direction. As discussed by Goldstein *et al.* (1998), absolute strains are critical for studies of mass transport and volume change during deformation. In the sample studied here, the spacing between S_1 foliation surfaces has increased during the D_2 deformation, and this could either be accomplished by ductile shape-change of material between the foliation planes, or by the addition of new material. The ability of OCM strain analysis to characterize heterogeneity in longitudinal strains also allows the worker to focus on specific areas that have undergone the greatest extension, and to look for evidence of intense deformation, or alternatively, of deposition of new material in these regions. Detailed analysis of OCM-bearing rocks may provide a means of mapping out regions of material gain or loss, and of mass-transport pathways during deformation. In particular, this method could be applied around fold hinges, where OCMs are most commonly preserved.

which may provide detailed information on folding mechanisms and volume redistribution during folding.

Quantitative strain studies using OCMs may provide new evidence about porphyroblast rotation relative to an externally-fixed reference frame during ductile deformation, which remains a lively and controversial topic (e.g. Bell *et al.*, 1992; Passchier *et al.*, 1992; Johnson, 1993, Johnson and Vernon, 1995; Bell and Hickey, 1997; Henderson, 1997). For example, all the porphyroblasts in the rock studied here appear to have grown at the same time in the deformation-metamorphic history (Bell and Rubenach, 1980; Johnson and Moore, 1996), but orientations of the straight inclusion trails vary over a relatively wide range compared to the enveloping surface for matrix S_i, which has a fairly uniform orientation from thin section to thin section (compare Fig. 3a & b). If such large variations in the original foliation orientation were present at the onset of the syn-OCM deformation, they should have been greatly accentuated in the matrix during deformation. Additionally, extension values measured in the X-direction from the OCMs should vary, reflecting the variation in the original orientation of the foliation. However, the uniform orientation of matrix S_i on the thin-section scale, and the very consistent elongation data, suggest that the inclusion trails and matrix S_i all had approximately the same orientation at the onset of the syn-OCM deformation. This in turn suggests rotation of porphyroblasts relative to one another during OCM development. A careful study of these rocks, documenting finite strains, the orientations of inequant porphyroblasts, the magnitudes of porphyroblast axial ratios, and the orientations of inclusion trails and matrix foliations, may provide new constraints on porphyroblast rotation during ductile deformation. Such a study should, if possible, be conducted with oriented samples collected around a meso- or macroscale fold formed during the same deformation responsible for the OCMs.

Acknowledgements This study was supported by an Australian Research Council Large Grant No. A39700451 and Queen Elizabeth II Research Fellowship (to Johnson). We thank T. H. Bell and M. J. Rubenach for the spectacular sample from the Robertson River Metamorphics, D. W. Durney for helpful discussions and W. D. Means and C. Teyssier for helpful reviews.

REFERENCES

Aerden, D. G. A. M. (1995) Porphyroblast non-rotation during crustal extension in the Variscan Lys Caillaouas Massif, Pyrenees. *Journal of Structural Geology* **17,** 709–725.

Beach, A. (1979) The analysis of deformed belemnites. *Journal of Structural Geology* **1,** 127–135.

Bell, T. H., Fleming, P. D. and Rubenach, M. J. (1986) Porphyroblast nucleation, growth and dissolution in regional metamorphic rocks as a function of deformation partitioning during foliation development. *Journal of Metamorphic Geology* **4,** 37–67.

Bell, T. H. and Hickey, K. A. (1997) Distribution of pre-folding linear indicators of movement direction around the Spring Hill Synform, Vermont: significant for mechanism of folding in this portion of the Appalachians. *Tectonophysics* **274,** 274–294.

Bell, T. H., Johnson, S. E., Davis, B., Forde, A., Hayward, N. and Wilkins, C. (1992) Porphyroblast inclusion-trail orientation data: eppure non son girate! *Journal of Metamorphic Geology* **10,** 295–307.

Bell, T. H. and Rubenach, M. J. (1980) Crenulation cleavage development—evidence of progressive bulk inhomogeneous shortening from the "millipede" microstructure in the Robertson River Metamorphics. *Tectonophysics* **68,** T9–T15.

Christensen, J. N., Rosenfeld, J. L. and DePaolo, D. J. (1989) Rates of tectonometamorphic processes from rubidium and strontium isotopes in garnet. *Science* **244,** 1465–1469.

Christensen, J. N., Selverstone, J., Rosenfeld, J. L. and DePaolo, D. J. (1994) Correlation by Rb–Sr geochronology of garnet growth histories from different structural levels within the Tauern Window, Eastern Alps. *Contributions to Mineralogy and Petrology* **118,** 1–12.

Davis, B. K. (1995) Regional-scale foliation reactivation and re-use during formation of a macroscopic fold in the Robertson River Metamorphics, north Queensland, Australia. *Tectonophysics* **242,** 293–311.

Fyson, W. K. (1980) Fold fabrics and emplacement of an Archean granitoid pluton, Cleft Lake, Northwest Territories. *Canadian Journal of Earth Sciences* **17,** 325–332.

Goldstein, A., Knight, J. and Kimball, K. (1998) Deformed graptolites, finite strain and volume loss during cleavage formation in rocks of the Taconic slate belt, New York and Vermont, USA. *Journal of Structural Geology* (in press).

Hanna, S. S. and Fry, N. (1979) A comparison of methods of strain determination in rocks from the southwest Dyfed (Pembrokeshire) and adjacent areas. *Journal of Structural Geology* **1,** 155–162.

Henderson, J. R. (1997) Development of a chevron cleavage pattern and porphyroblast rotation in graded metaturbidites, Slave structural province, Northwest Territories, Canada. *Journal of Structural Geology* **19,** 653–661.

Johnson, S. E. (1990) Deformation history of the Otago schists, New Zealand, from progressively developed porphyroblast-matrix microstructures: uplift–collapse orogenesis and its implications. *Journal of Structural Geology* **12,** 727–746.

Johnson, S. E. (1993) Testing models for the development of spiral-shaped inclusion trails in garnet porphyroblasts: to rotate or not to rotate, that is the question. *Journal of Metamorphic Geology* **11,** 635–659.

Johnson, S. E. and Bell, T. H. (1996) How useful are 'millipede' and other similar porphyroblast microstructures for determining syn-metamorphic deformation histories? *Journal of Metamorphic Geology* **14,** 15–28.

Johnson, S. E. and Moore, R. R. (1996) De-bugging the 'millipede' porphyroblast microstructure: a serial thin-section study and 3-D computer animation. *Journal of Metamorphic Geology* **14,** 3–14.

Johnson, S. E. and Vernon, R. H. (1995) Inferring the timing of porphyroblast growth in the absence of continuity between inclusion trails and matrix foliations: can it be reliably done? *Journal of Structural Geology* **17,** 1203–1206.

Lanzirotti, A. and Hanson, G. N. (1997) An assessment of the utility of staurolite in U–Pb dating of metamorphism. *Contributions to Mineralogy and Petrology* **129,** 352–365.

Passchier, C. W. and Speck, P. J. H. R. (1994) The kinematic interpretation of obliquely-transected porphyroblasts: an example from the Trois Seigneurs Massif, France. *Journal Structural Geology* **16,** 971–984.

Passchier, C. W., Trouw, R. A. J., Zwart, H. J. and Vissers, R. L. M. (1992) Porphyroblast rotation: eppur si muove? *Journal of Metamorphic Geology* **10,** 283–294.

Ramsay, J. G. and Huber, M. I. (1983) *The Techniques of Modern Structural Geology, Volume 1: Strain Analysis*. Academic Press, London.

Spear, F. S. (1993) Metamorphic Phase Equilibria and Pressure–Temperature–Time Paths. Mineralogical Society of America, Monograph 1. Bookcrafters, Inc., Michigan, U.S.A.

Vance, D. and O'Nions, R. K. (1992) Prograde and retrograde thermal histories from the central Swiss Alps. *Earth and Planetary Science Letters* **114,** 113–129.

Vernon, R. H. (1989) Porphyroblast-matrix microstructural relationships: recent approaches and problems. In *Evolution of Metamorphic Belts*, eds J. S. Daly, R. A. Cliff and B. W. D. Yardley, pp. 83–102. Geological Society Special Publication **43.**

Williams, M. L. (1994) Sigmoidal inclusion trails, punctuated fabric development, and interactions between metamorphism and deformation. *Journal of Metamorphic Geology* **12,** 1–21.

Zwart, H. J. (1962) On the determination of polymetamorphic mineral associations and its application to the Bosost area (Central Pyrenees). *Geologische Rundschau* **52,** 38–65.